Type of the Paper (Article)

Lysine methyl transferase inhibitors impair H4K20me2 and 53BP1 foci in response to DNA damage in sarcomas, a synthetic lethality strategy

Ignacio Campillo-Marcos[1,2,(ORCID: 0000-0002-7657-7127)] , **Eva Monte-Serrano**[1,2,(ORCID: 0000-0002-0865-2244)], **Elena Navarro-Carrasco**[1,2,(ORCID: 0000-0002-1533-8210)] , **Raúl García-González**[1,2, (ORCID: 0000-0003-4044-2543)] , **and Pedro A. Lazo**[1,2, (ORCID: 0000-0001-8997-3025)] *

[1] Molecular Mechanisms of Cancer Program, Instituto de Biología Molecular y Celular del Cáncer, Consejo Superior de Investigaciones Científicas (CSIC)-Universidad de Salamanca, 37007 Salamanca, Spain; ignacio_cm@usal.es (I. C.-M.); evamonte26@usal.es (E. M.-S.); elena.navarro@usal.es (E. N.-C.); garcia-raul@usal.es (R. G.-G.); pedro.lazo@csic.es (P. A. L.)

[2] Instituto de Investigación Biomédica de Salamanca (IBSAL), Hospital Universitario de Salamanca, 37007 Salamanca, Spain.

* Correspondence: pedro.lazo@csic.es

Simple summary: Epigenetic modification of histones modulates chromatin remodeling. In this report, we have tested the effect of two lysine methyltransferase inhibitors, chaetocin and tazemetostat, on the DNA damage response in sarcoma cells. These inhibitors facilitate chromatin relaxation and DNA damage, which were detected by the increase of H4K16ac levels and the labeling of free DNA-ends and γH2AX foci. Moreover, they block the DDR at specific repair steps, both by preventing the accumulation of H4K20me2, and the recruitment of 53BP1 to damaged DNA. These KMT inhibitors facilitate tumor cell death detected by the processing of caspase 3 and PARP1. Therefore, KMT inhibitors can be used in synthetic lethality strategies in combination with doxorubicin or ionizing radiation in sarcomas.

Abstract. Background: Chromatin is dynamically remodeled to adapt to all DNA-related processes, including DNA damage responses (DDR). This adaptation requires DNA and histone epigenetic modifications, which are mediated by several types of enzymes; among them are lysine methyltransferases (KMTs). **Methods:** KMT inhibitors, chaetocin and tazemetostat (TZM), were used to study their role in the DDR induced by ionizing radiation or doxorubicin in two human sarcoma cells lines. The effect of these KMT inhibitors was tested by the analysis of chromatin epigenetic modifications, H4K16ac and H4K20me2. DDR was monitored by the formation of γH2AX, MDC1, NBS1 and 53BP1 foci, and the induction of apoptosis. **Results:** Chaetocin and tazemetostat treatments caused a significant increase of H4K16 acetylation, associated with chromatin relaxation; and increased DNA damage, detected by the labeling of free DNA-ends. These inhibitors significantly reduced H4K20 dimethylation levels in response to DNA damage and impaired the recruitment of 53BP1, but not of MDC1 and NBS1, at DNA damaged sites. This modification of epigenetic marks prevents DNA repair by the NHEJ pathway and leads to cell death. **Conclusion:** KMT inhibitors can function as sensitizers to DNA damage-based therapies and be used in novel synthetic lethality strategies for sarcoma treatment.

Keywords: chaetocin, tazemetostat, ionizing radiation, doxorubicin, DNA repair, γH2AX, 53BP1, histone H4.

1. Introduction

Chromatin structure is dynamically remodeled by DNA and histone epigenetic modifications to control and coordinate all DNA-based processes such as transcription, replication, recombination or DNA repair [1,2]. These epigenetic modifications are mediated by several chromatin modifiers and depend on the cellular context [3-6]. Some of these proteins that modify, or bind to, histone modifications are often dysregulated in cancer and have been used as drug targets in novel therapeutic strategies in oncology [6].

Histone methylation is one of the most prevalent chromatin modifications and plays a key role in the regulation, activation and silencing of genes in euchromatin, and is also associated with heterochromatin condensation [6]. This dynamic covalent modification of histones occurs in N-terminal lysine or arginine residues [7,8], and several inhibitors have been designed against lysine methyltransferases (KMTs) and demethylases (KDMs), which can be used to improve current cancer treatments [9,10]. Among them is chaetocin, which inhibits KMTs such as SUV39H1 [11-13] or G9a [14,15]. In addition to its role as KMT inhibitor [11], chaetocin is also a competitive inhibitor of thioredoxin reductase, whose function is to compensate the deleterious effect of reactive oxygen species (ROS) [16]. Furthermore, other exogenous agents such as ionizing radiation also facilitate ROS production [17,18], causing single- and double-strand breaks (SSBs and DSBs, respectively) [17], and their accumulation can lead to cell death [17]. Both effects contribute to chromatin relaxation and the generation of oxidative stress, which facilitate DNA damage [16,19-21]. In this context, chaetocin also induces cell death in different types of tumors, including multiple myeloma [21], leukemia [12], melanoma [22], gliomas [19,23], and gastric [24], ovarian [25], and non-small cell lung cancers [26]. Another recent KMT inhibitor that targets EZH2 is tazemetostat, which is clinically used in sarcomas [27,28]. Furthermore, PARP1 regulates NHEJ (Non-homologous end joining) [29,30], and its inhibitors, such as olaparib, also cause DNA damage [31], which in combination with DNA damaging agents, such as ionizing radiation (IR), is also used in sarcomas [32].

SSBs and DSBs are specifically repaired by different DDR mechanisms, which are strictly coordinated in order to sequentially detect, identify, signal and repair specific DNA lesions based on their type [18,33]. Initially, all these DDR pathways require a local distortion of chromatin caused by the DNA lesion [34,35], which is necessary to trigger the sequential steps in the response, ranging from chromatin remodeling and DNA protection of damaged sites, to the recognition of the type of damage and the activation of the corresponding specific DDR pathway [36,37]. These sequential processes involve changes in covalent modifications of histones [36], which are necessary for the recruitment of specific DNA repair factors. In this context, histone acetylation plays an important role in response to DNA damage, since acetylated histones H3 and H4 are recognized by chromatin remodelers and protein kinases implicated in specific DDR pathways [38,39]. The acetylation of histone H4 in K16 (H4K16ac) is also induced in response to DNA damage and is associated with chromatin relaxation [39,40]. However, other chromatin readers depend on specific histone methylations to be recruited to DNA damage sites, such as 53BP1 [41-

43], a protein involved in non-homologous end joining (NHEJ) [44-46], a key DNA repair pathway in resting cells such as neurons or cancer stem cells. In this context, the dimethylation of histone H4 in lysine 20 (H4K20me2), mediated by SET8 [47] and MMSET [48], is necessary for the recruitment of 53BP1 at locations with DNA damage [41,47]. H4K20me2 stabilizes the interaction between chromatin and 53BP1 in foci [49], and facilitate DNA repair by the NHEJ pathway [44,50].

Due to the role of DDR in the maintenance of genome integrity and cellular homeostasis, defects in DNA repair pathways directly lead to the accumulation of SSBs and DSBs, and the subsequent cell death. In fact, patients with mutations in several DDR pathways respond much better to treatment, becoming super responders [51]. In this work, we have studied the molecular base by which KMT inhibitors, chaetocin and tazemetostat, impair DDR [32, 52] by mimicking a DNA repair defect, could be used as DNA damage sensitizers [53, 54] and become candidates for synthetic lethality strategies in sarcomas cells treated with either ionizing radiation (IR) [32] or doxorubicin [52,55].

2. Results

2.1. Chaetocin induces DNA damage by itself and impairs the recruitment of 53BP1 at damage sites

Initially, we tested whether chaetocin, a KMT inhibitor, is able to induce DNA damage, which was detected by the formation of γH2AX foci, a surrogate marker of DDR early steps [56-58]. Chaetocin significantly increased the number of γH2AX foci with respect to control cells (Fig. 1A, B). However, the combination of this inhibitor with different doses of ionizing radiation (IR), another source of oxidative stress, did not show a synergic effect on the assembly of these foci in U2OS osteosarcoma cells (Figure 1A, B, C) and SK-LMS-1 leiomyosarcoma cells (Supplementary Figure S2). These data suggested that both, chaetocin and IR, by themselves have already reached their maximum effect.

After the initial phosphorylation of histone H2AX, additional repair proteins are sequentially recruited to DSBs. One of these proteins is 53BP1 [41,42], which determines DNA repair by the NHEJ pathway [43,59]. We studied whether chaetocin interferes with the assembly of 53BP1 foci in serum-deprived cells. The formation of these 53BP1 foci was impaired in U2OS osteosarcoma cells treated with chaetocin, independently of the dose of IR used (Figure 1B, C). No differences in 53BP1 protein levels were detected by western blot after chaetocin and/or IR treatments (Figure 1D), which rules out a reduction of endogenous 53BP1 protein, as the cause of foci loss. Similar results were obtained in SK-LMS-1 leiomyosarcoma cells (Supplementary Figure S2) Therefore, we concluded that chaetocin impairs the recruitment of 53BP1, but not of γH2AX, to DSBs induced by IR.

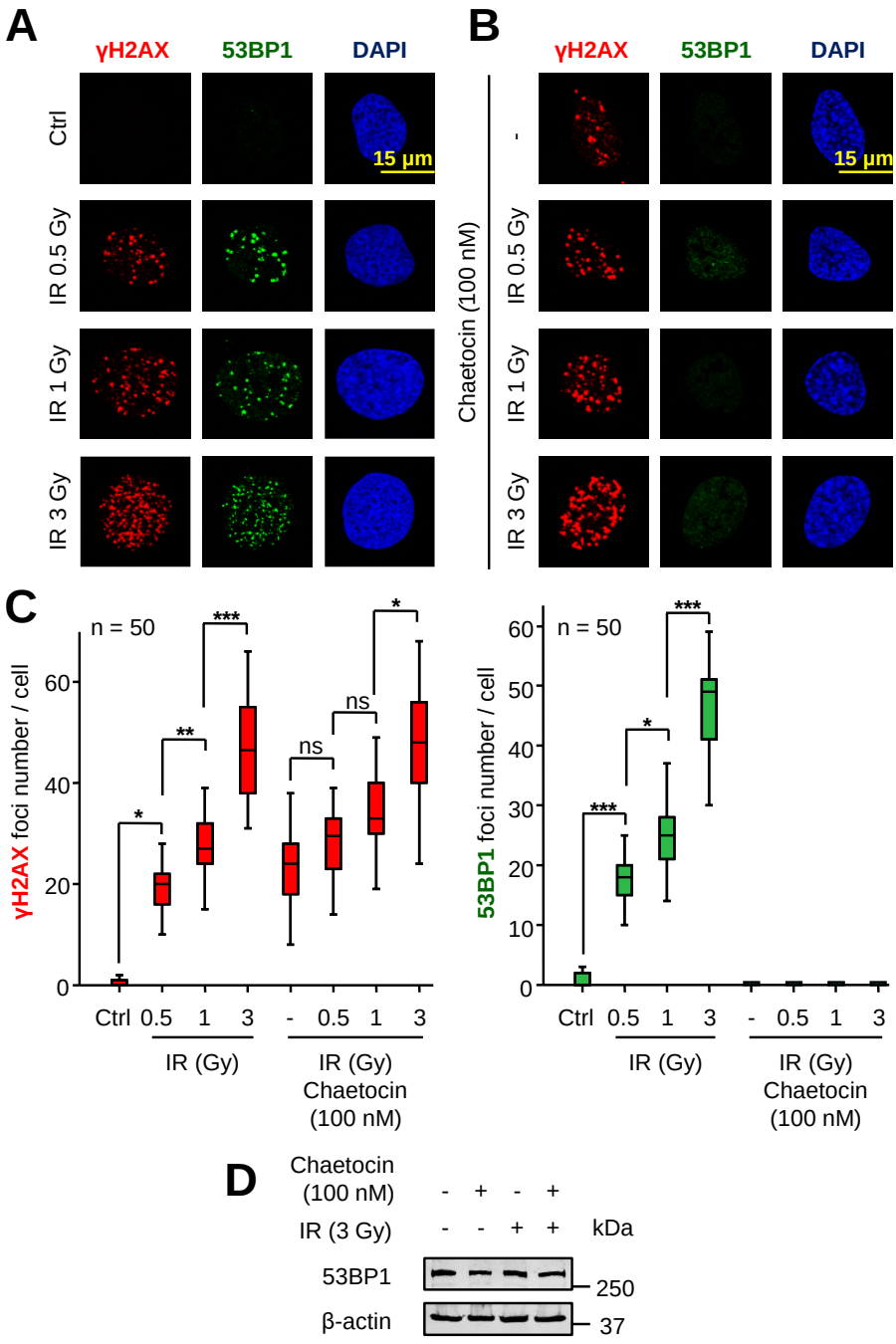

Figure 1. Chaetocin impairs the assembly of 53BP1 foci in response to ionizing radiation (IR) in U2OS cells deprived of serum. **A**. γH2AX and 53BP1 foci formation in response to different doses of IR. **B**. Effect of chaetocin on γH2AX and 53BP1 foci formation after inducing DNA damage with different doses of IR. **C**. Quantification of γH2AX (left) and 53BP1 (right) foci in response to chaetocin and/or IR. **D**. The immunoblot shows that chaetocin and/or IR have no effect on 53BP1 protein levels. ns: not significant. * $p < 0.05$, ** $p < 0.01$, *** $p < 0.001$. These images only show the detail in one cell selected for presentation. The field images are shown in Supplementary Figure S1.

2.1. Chaetocin induces DNA damage by itself and impairs the recruitment of 53BP1 at damage sites

Initially, we tested whether chaetocin, a KMT inhibitor, is able to induce DNA damage, which was detected by the formation of γH2AX foci, a surrogate marker of DDR early steps [56-58]. Chaetocin significantly increased the number of γH2AX foci with respect to control cells (Fig. 1A, B). However, the combination of this inhibitor with different doses of ionizing radiation (IR), another source of oxidative stress, did not show a synergic effect on the assembly of these foci in U2OS osteosarcoma cells (Figure 1A, B, C) and SK-LMS-1 leiomyosarcoma cells (Supplementary Figure S2). These data suggested that both, chaetocin and IR, by themselves have already reached their maximum effect.

After the initial phosphorylation of histone H2AX, additional repair proteins are sequentially recruited to DSBs. One of these proteins is 53BP1 [41,42], which determines DNA repair by the NHEJ pathway [43,59]. We studied whether chaetocin interferes with the assembly of 53BP1 foci in serum-deprived cells. The formation of these 53BP1 foci was impaired in U2OS osteosarcoma cells treated with chaetocin, independently of the dose of IR used (Figure 1B, C). No differences in 53BP1 protein levels were detected by western blot after chaetocin and/or IR treatments (Figure 1D), which rules out a reduction of endogenous 53BP1 protein, as the cause of foci loss. Similar results were obtained in SK-LMS-1 leiomyosarcoma cells (Supplementary Figure S2) Therefore, we concluded that chaetocin impairs the recruitment of 53BP1, but not of γH2AX, to DSBs induced by IR.

The lack of 53BP1 foci in response to the combination of IR and chaetocin might be a consequence of a delay in the assembly of these foci caused by chaetocin, which might require longer times. Because of that, we performed a time curve after chaetocin treatment and/or IR exposure and analyzed both γH2AX and 53BP1 foci formation at different time points. We observed that 53BP1 foci did not assemble in response to chaetocin independently of the post-irradiation time, but this protein was diffusely accumulated in nuclei. However, the number and size of γH2AX residual foci (12 hours post-IR) increased significantly (Supplementary figure S3). These results demonstrated that DDR is not working efficiently in presence of chaetocin, implying that the sequential response is blocked. Consequently, earlier proteins participating in this process, such as γH2AX, are accumulated at DNA damaged sites, whose repair is stalled.

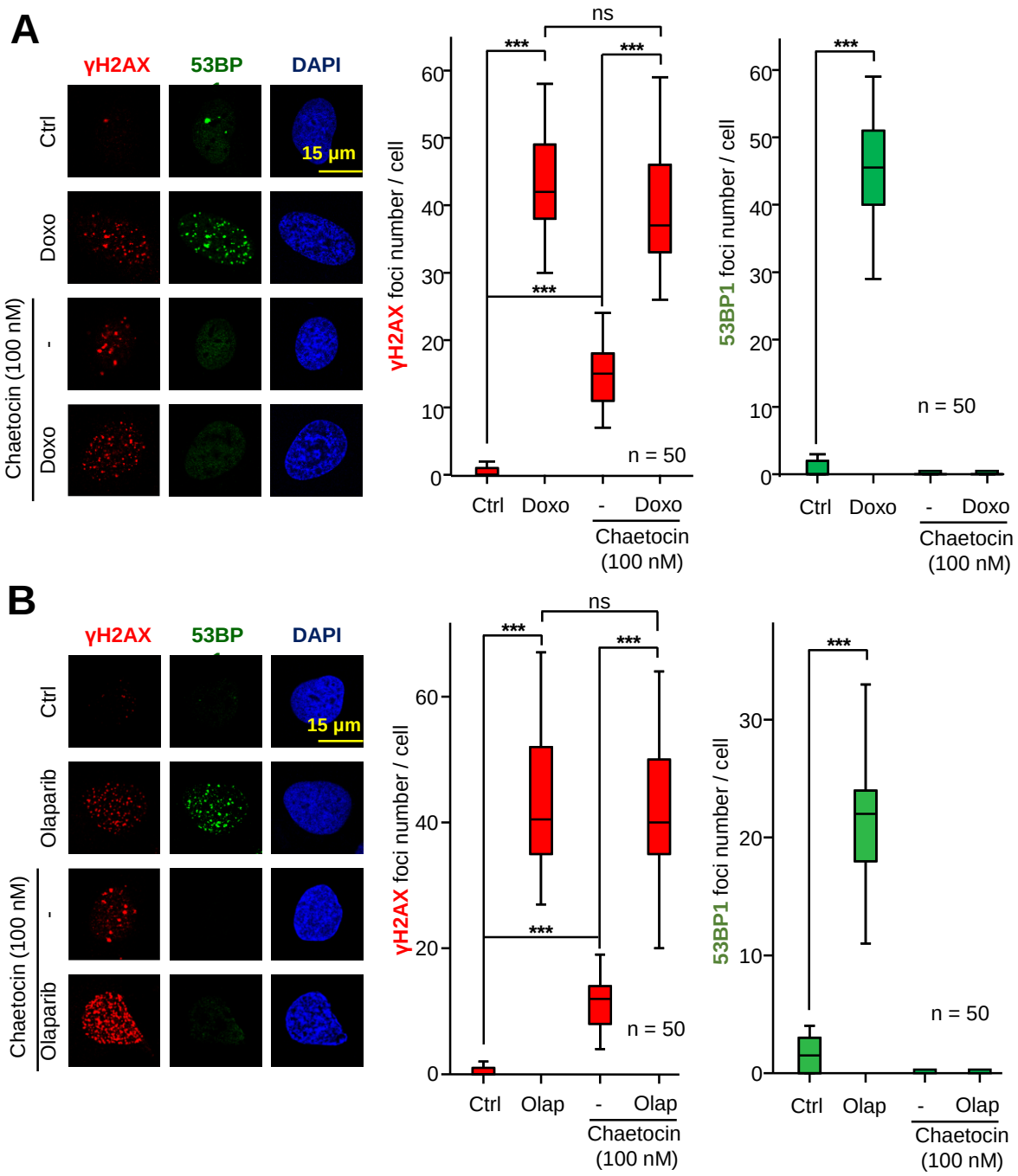

Figure 2. Effect of chaetocin on the formation of γH2AX and 53BP1 foci after inducing DSBs with doxorubicin (Doxo) (**A**) and olaparib (Olap) (**B**) in U2OS cells deprived of serum mitogenic signals. The effect of chaetocin on these foci in response to IR in SK-LMS-1 cells is shown in Supplementary Figure S2. Quantifications of these nuclear foci in response to chaetocin and/or doxorubicin are shown to the right. ns: not significant, *** $p < 0.001$.

2.3. MDC1 and NBS1, intermediate DDR proteins between γH2AX and 53BP1 foci formation, are not affected by chaetocin treatment

The defective formation of 53BP1 foci might be a consequence of a disruption of previous steps in the sequential response to IR. Among them is the assembly of MDC1 and NBS1 foci, two proteins that are phosphorylated in response to IR, and mediate the accumulation of 53BP1 at DSBs [64-66]. To determine whether chaetocin impairs the formation of MDC1 and NBS1 foci, cells were treated with chaetocin, DNA damage was induced by IR, and the formation of MDC1 and NBS1 foci was studied. Chaetocin did not interfere with either MDC1 (Figure 3A) or NBS1 foci formation (Figure 3B) in response to IR, which are two sequential steps between γH2AX and 53BP1 foci in DDR, but their protein levels were not affected. This suggests that this DDR failure is due to the deficient recruitment of 53BP1 at locations with damaged DNA as a consequence of chaetocin treatment.

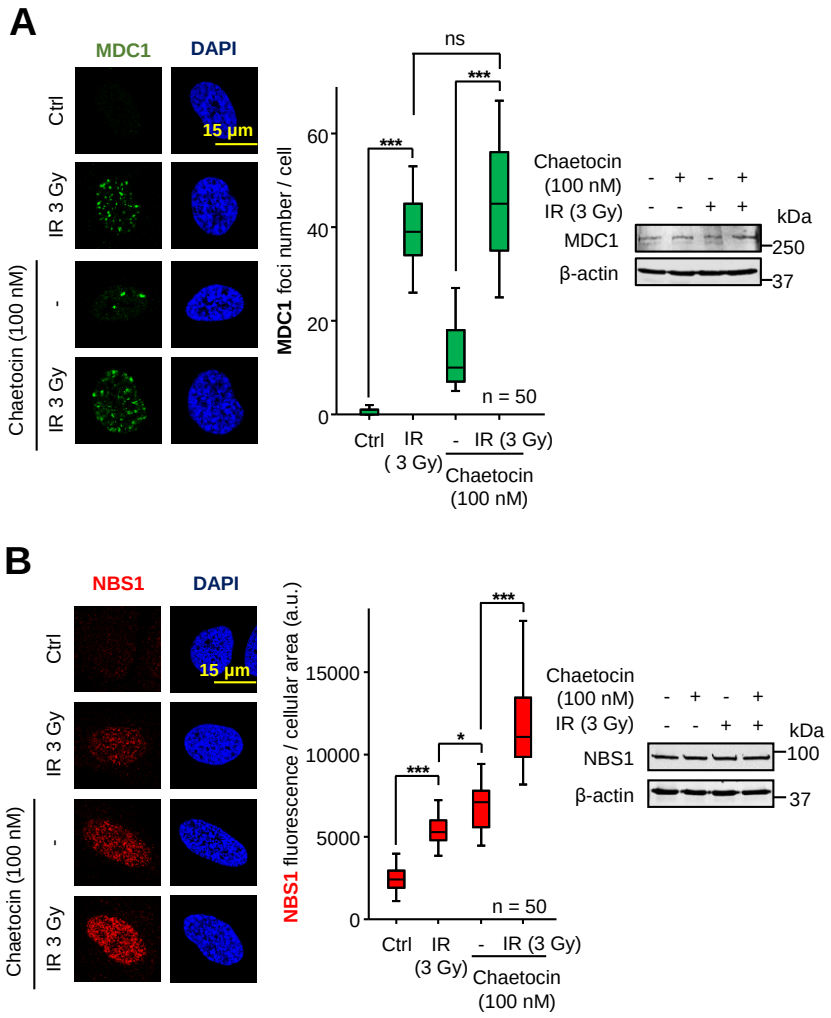

Figure 3. Chaetocin does not interfere with MDC1 foci formation after inducing DSBs by IR in U2OS cells deprived of serum. **A**. Effect of chaetocin on MDC1 foci in response to IR (3 Gy). Quantification of MDC1 foci after treating cells with chaetocin, IR and their combination (center). The immunoblot reflects that no variations in MDC1 protein levels are induced by chaetocin and/or IR (right). ns: not significant. *** $p < 0.001$. **B.** Effect of chaetocin on NBS1 accumulation in response to IR (3 Gy) in U2OS cells. Quantification of NBS1 nuclear fluorescence after treating cells with chaetocin, IR and their combination (center). The immunoblot reflects that no variations in NBS1 protein levels were induced by chaetocin and/or IR (right). ns: not significant, * $p < 0.05$, *** $p < 0.001$.

2.4. H4K20me2 induced by DNA damage are impaired by chaetocin treatment

One of the chromatin modifications that mediates the recruitment of 53BP1 at DSBs is the dimethylation of the histone H4 at lysine 20 (H4K20me2), which is directly recognized by the TUDOR domains of 53BP1 [41,67]. Therefore, we tested the ability of chaetocin to modify H4K20me2 levels in response to IR or doxorubicin in U2OS and SK-LMS-1 sarcoma cells. The treatment of both cell lines with the combination of chaetocin and IR resulted in a significant reduction of H4K20me2 levels (Figure 4A, Supplementary figure S4A). Furthermore, this reduction in H4K20 dimethylation levels was also observed in response to doxorubicin and chaetocin treatments (Figure 4B, Supplementary figure S4B). This effect on H4K20me2 explains why this KMT inhibitor only affects the accumulation of 53BP1, but not of γH2AX, NBS1 or MDC1 at damaged sites.

DNA damage causes an early local relaxation of chromatin that is associated with the acetylation of histone H4 in K16 (H4K16ac) [39,68]. Therefore, we also determined H4K16 acetylation levels, which have to decrease in order to enable 53BP1 to bind to chromatin through H4K20me2 [45,69]. As expected, these H4K16 acetylation levels increased after inducing DNA damage by IR and, in a smaller degree, by chaetocin, since this modification is a very early step in DDR, but such high levels remain high in response to the combination of IR and chaetocin (Supplementary Figure S5). These data reinforce the idea that KMT inhibitors like chaetocin involve changes in the histone epigenetic code that interfere with DNA repair by the NHEJ pathway.

2.5. Tazemetostat impairs H4K20me2 the DNA Damage Response induced by doxorubicin

Since tazemetostat is a KMT inhibitor currently used in clinical practice, we tested whether tazemetostat could also impair the H4K20me2 as part of the DDR in cells treated with doxorubicin. The treatment of U2OS (Figure 5A) and SK-LMS-1 (Figure 5B) cells with tazemetostat significantly reduced H4K20me2 levels and the formation of γH2AX and 53BP1 foci induced by doxorubicin in both sarcoma cell lines (Supplementary Figure S6; Supplementary Figure S7).

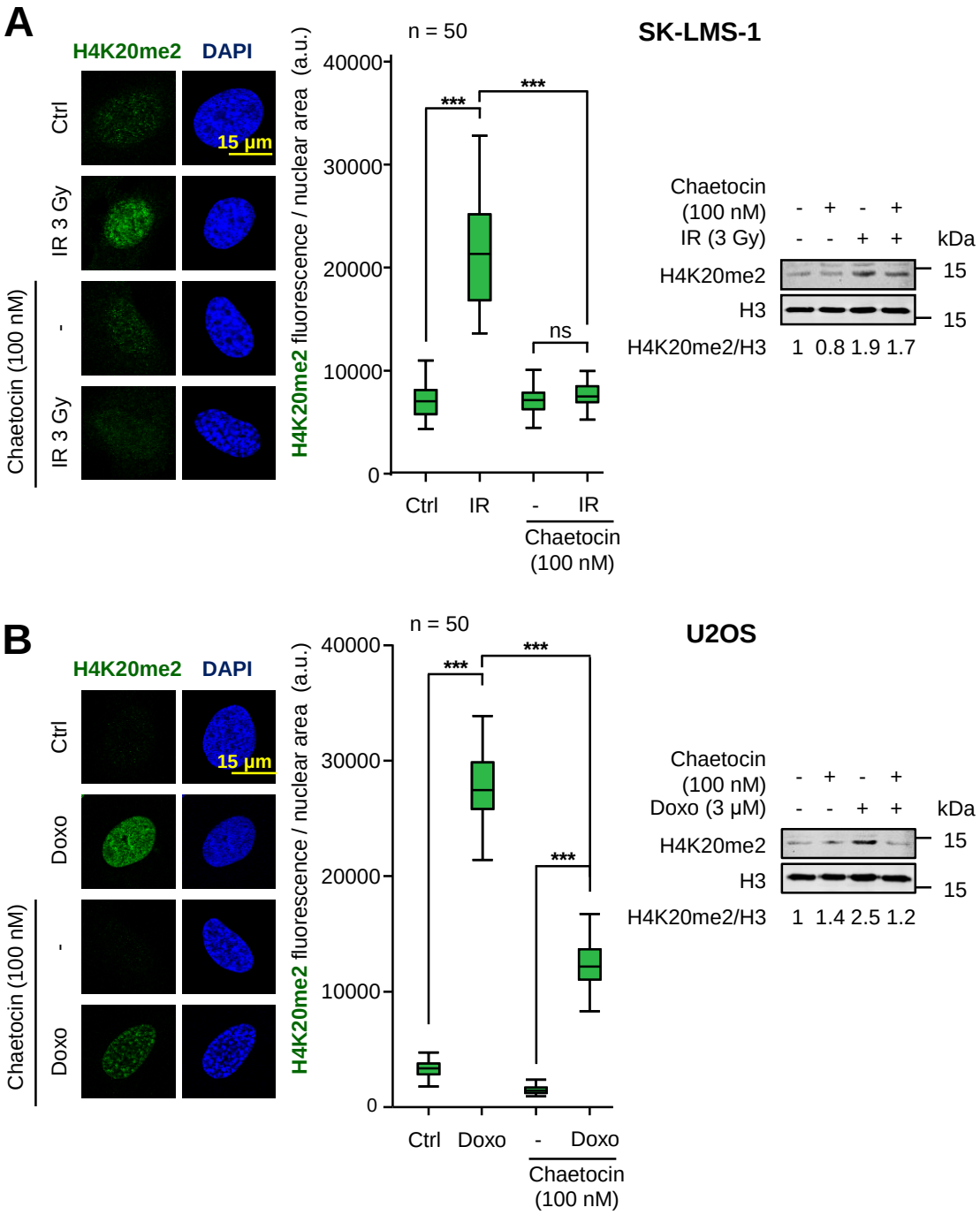

Figure 4. Effect of chaetocin on H4K20me2 induced by IR or doxorubicin. **A.** Effect of chaetocin on H4K20me2 induced by IR in SK-LMS-1 cells. **B.** Effect of chaetocin on H4K20me2 induced by doxorubicin (Doxo) in U2OS cells. Quantification of nuclear fluorescence associated with H4K20 dimethylation in response to chaetocin, IR, doxorubicin or their combination (center). Analysis of H4K20me2 levels by western blot (right). ns: not significant, *** $p < 0.001$.

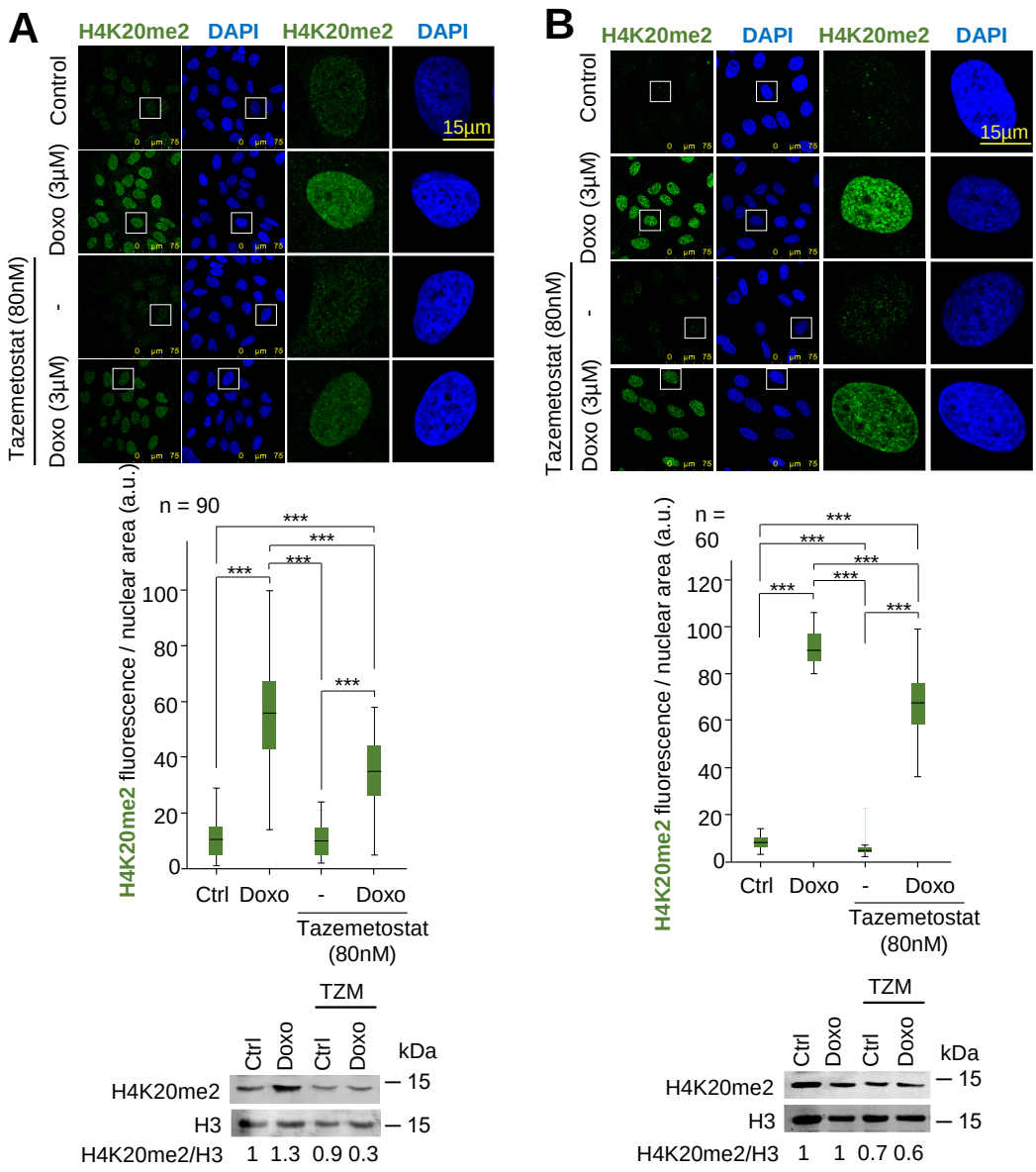

Figure 5. Effect of tazemetostat (TZM) on H4K20me2 levels in response to DNA damage induced by doxorubicin. **A.** Effect of tazemetostat on the levels of H4K20me2 in U2OS cells deprived of serum. The tazemetostat effect on γH2AX and 53BP1 is shown in Supplementary Figure S6. **B.** Effect of tazemetostat on the levels of H4K20me2 in SK-LMS-1 cells. The tazemetostat effect on γH2AX and 53BP1 is shown in Supplementary Figure S7. *** $p < 0.001$.

2.6. JMJD2 inhibitor does not alter the formation of 53BP1 foci induced by DNA damage

53BP1 is an essential mediator protein in NHEJ pathway and its recruitment at damage sites depends on covalent modifications in specific histones residues and repair proteins. Since chaetocin or tazemetostat, KMT inhibitors, impair the accumulation of 53BP1 at damage sites in response to DNA damage, we studied the consequences of treatment with a lysine demethylase (KDM) inhibitor, JMJD2i, on 53BP1 foci formation. Our results showed that these foci were correctly formed after the combination of JMJD2i and different doses of IR (Supplementary Figure S8). This result confirms that the effect of chaetocin

and tazemetostat on 53BP1 foci formation is modulated by variations in the methylation pattern of histones.

2.7. Chaetocin and tazemetostat facilitate DNA damage induced by doxorubicin

A consequence of KMT inhibition would be a facilitation of chromatin relaxation, which makes tumor cells more susceptible to undergo DNA damage. Tazemetostat is a new KMT inhibitor that targets EZH2 and G9a [70,71] that has been approved for the treatment of sarcomas [72]. Therefore, we tested whether these two KMT inhibitors, chaetocin and tazemetostat, can really cause DNA damage by themselves or in cooperation with doxorubicin. The accumulation DNA damage was detected by labelling nuclear free-DNA ends in a TUNEL assay. These two KMT inhibitors by themselves caused a minor, but significant increase in DNA damage, which reached their maximum effect when they were combined with doxorubicin in both U2OS (Figure 6A) and SK-LM-1 cells (Figure 6B)

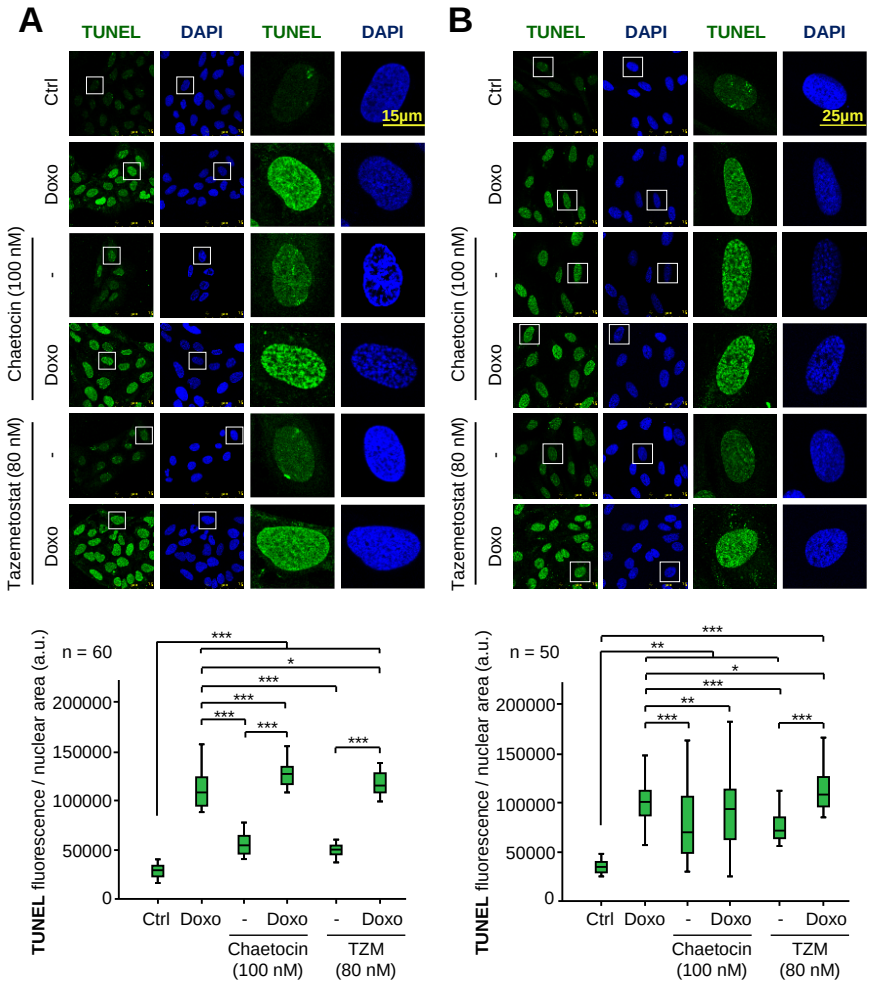

Figure 6. Effect of chaetocin and tazemetostat on induction of DNA damage detected in TUNEL assays in U2OS **(A)** and SK-LMS-1 **(B)** sarcoma cells deprived of serum. DNA damage was detected by labelling free DNA ends. * $p < 0.05$, ** $p < 0.01$, *** $p < 0.001$.

2.8. Chaetocin and tazemetostat promote cell death in response to DNA damage induction

Next, we analyzed the effect of these inhibitors, chaetocin and tazemetostat, on the induction of apoptosis by detection of the cleavage of caspase 3 and PARP1. PARP1 is cleaved by activated caspase 3 and can be detected as a smaller protein with a specific antibody for this cleaved fragment.. Because of that, the cleavage of caspase-3 and PARP1 was determined in both sarcoma cell lines. Cleaved caspase 3 was detected after chaetocin or tazemetostat treatments either by themselves or in combination with doxorubicin at different time points in both cell lines (Figure 7A, B). Chaetocin by itself was able to induce caspase activation at shorter times than tazemetostat, whose effect required a longer time and the cooperation of doxorubicin. The processing of PARP1 as a result of caspase activation was similarly determined (Figure 7C, D). Chaetocin was also more effective at a shorter time than tazemetostat and PARP1 processing that was induced by these drugs in cooperation with doxorubicin. This effect of chaetocin on PARP1 processing induced by ionizing radiation was further confirmed in U2OS and SK-LMS cell lines (Supplementary Figure S9).

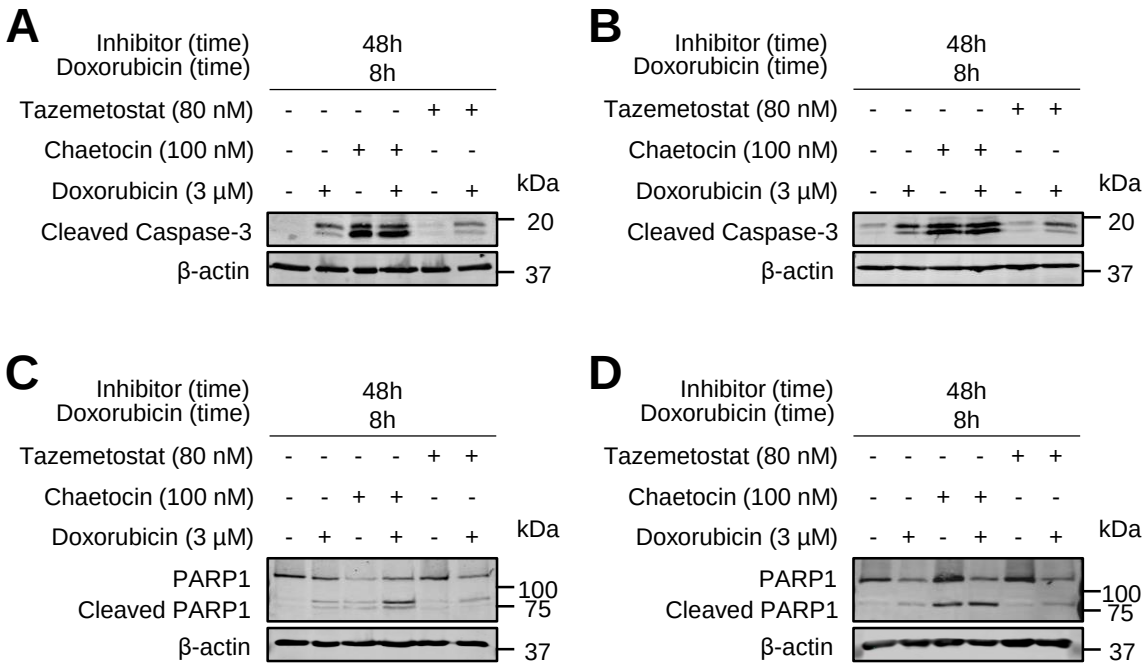

Figure 7. Chaetocin and tazemetostat cause an activation of caspases detected by the processed caspase 3 and PARP1 in doxorubicin treated cells. Effect of chaetocin and tazemetostat on processed caspase 3 after treatment with doxorubicin in U2OS **(A)** and SK-LMS-1 **(B)** cells deprived of serum. Effect of chaetocin and tazemetostat on PARP1 cleavage after treatment with doxorubicin in U2OS **(C)** and SK-LMS-1 **(D)** cells deprived of serum. The cleavage of PARP1 in response to chaetocin is shown in Supplementary Figure S9.

3. Discussion

Genomic instability contributes to cancer development. However, the generation of excessive DNA damage by treatment combinations can lead to a loss of tumor cell viability. In this context, approaches promoting DNA damage accumulation in tumor cells can be exploited in novel cancer therapeutic strategies of synthetic lethality. Among potential targets are those proteins involved in different DDR pathways either by combining them in tumors with mutations in a DDR gene, such as BRCA1 [61] or WRN [73-75], or by pharmacological targeting of another DDR pathway, such as olaparib, which targets PARP1 [76-78]. An alternative is to simultaneously targeting two different DDR pathways, or associated processes such as chromatin remodeling, with drugs to promote tumor cell death. Based on that, KMTs are good candidates, since they regulate chromatin compaction. If these KMT inhibitors are combined with DNA-based treatments, such as IR or doxorubicin, which are commonly used in sarcomas, the impact on DNA damage can be significantly higher and thus lethal for the tumor cell.

The recruitment of 53BP1 to chromatin in response to DSBs depends on two major components. One is the balance of epigenetic modifications such as H4K16ac [39,40] and H4K20me2 [67,79]. The other is the sequential accumulation and phosphorylation of histone γH2AX, MDC1 and NBS1 at DNA damaged locations [64-66,80,81] In this context, the inhibition of KMTs can interfere with DDR and the NHEJ pathway, which require the spatial and temporal coordination of different DNA repair factors and a local dynamic remodeling of chromatin. Therefore, the manipulation of epigenetic modifications mediated by the KMT inhibitors chaetocin and tazemetostat did not alter earlier steps in DDR, such as γH2AX, MDC1 and NBS1 foci, suggesting that KMT inhibitors have to work at later steps in DDR.

The dimethylation of histone H4 in lysine 20 (H4K20me2) stabilizes the interaction between chromatin and 53BP1 in foci [49]. Our study shows that chaetocin and tazemetostat strongly reduce H4K20me2 levels, and thus would interfere with DDR due to the impairment of 53BP1 recruitment to damage locations. Chaetocin is more efficient than tazemetostat in impairing H4K20me2, which is necessary for DDR by the NHEJ pathway. This effectiveness of chaetocin is likely to be a consequence of it less specific inhibition of KMTs, while tazemetostat has a more specific target, EZH2 [27,82,83]. Furthermore, the acetylation of H4K16 has to be removed in order to facilitate the dimethylation of H4K20 after the generation of DNA damage [69,84]. However, H4K16ac levels were still high in response to IR and chaetocin, making more difficult that H4K20 can be methylated and impairing 53BP1 recruitment to DNA damage locations. Both chaetocin and tazemetostat cause DNA damage by themselves, but this effect is particularly higher in the case of chaetocin. This effect is a likely consequence of the generation of oxidative stress by chaetocin, which is a competitive substrate, and inhibitor, of the thioredoxin reductase [16] leading to an increase of reactive oxygen species (ROS) that has been related to cell death, taking into account that oxidative stress is directly related to DNA damage [12,20-23,25,85-88]. This effect of on ROS and its lower KMT specificity make chaetocin more toxic than tazemetostat.

Due to the DDR impairment caused by KMT inhibitors, chaetocin or tazemetostat, DNA damage is accumulated and lead to tumor death. The treatment with these two KMT inhibitors caused an increase in DNA damage, higher when cells were treated with IR or doxorubicin, which was detected by labelling of free DNA-ends in TUNEL assays, and an increase in processed PARP1 and caspase-3, which indicates that apoptosis has been activated in tumor cells. All these results are consistent with the role of these KMT inhibitors in facilitating cell death [89,90].

Therefore, the combination of a KMT inhibitor with current treatments based on DNA damage in sarcomas, such as ionizing radiation or doxorubicin, can be useful to develop novel strategies that sensitize tumor cells and, at the same time, might contribute to reduce the dose of these toxic treatments. The consequence would be a reduction of treatment side effects that can lead to an improvement in patient quality of life and life expectancy.

4. Materials and methods

4.1. Reagents and Inhibitors

Doxorubicin (Ref. 16416646, Thermo-Fisher Scientific); olaparib (Ref. O-9201, LC Laboratories, Woburn, MA, USA), chaetocin (Ref. C9492, Sigma-Aldrich Merck), Tazemetostat (Ref. S7128, Selleckchem) and JMJD2 inhibitor (Ref. 420201, Calbiochem, Merck-Millipore). All other reagents were from Sigma-Aldrich-Merck (Darmstadt, Germany) (Supplementary Table S1).

4.2. Cell lines and culture

Two human sarcoma cell lines, U2OS (ATCC, HTB-96) from an osteosarcoma and SK-LMS-1 (ATCC, HTB-88) from a leiomyosarcoma, were obtained from the ATCC and grown as recommended by the supplier in DMEM supplemented with antibiotics, 10% FBS and 5 mM glutamine. Both cell lines are mycoplasma free. Experiments with inhibitors were performed in serum deprived cells for 48 hours to eliminate mitogenic signals.

4.3. DNA damage

DNA damage was induced by treatment with different doses (0.5, 1 or 3 Gy) of ionizing radiation using a Gammacell 1000 Elite irradiator (Theratronics, Ottawa, Canada) with a ^{137}Cs source. Alternatively DNA damage was also induced by treatment with doxorubicin or olaparib (PARP1 inhibitor) [91,92]. These measurements were performed in serum deprived cells (0.5%) for 48 hours to remove mitogenic signaling and promote DNA repair by the NHEJ pathway. Chaetocin (100 nM) or tazemetostat (80 nM) were added at 24 hours after serum withdrawal. DNA damage was induced by addition of either olaparib (10 μM) at 27 hours, doxorubicin (3 μM) at 46 hours, or ionizing radiation (IR) treatments at 48 hours.

4.4. Cell lysates and histone extraction

Cells were lysed with the RIPA lysis buffer (150 mM NaCl, 1.5 mM $MgCl_2$, 10 mM NaF, 4 mM EDTA, 50 mM Hepes, 1% Triton X-100, 0.1% SDS), and 10% glycerol) supplemented by phosphatases inhibitors (1 mM NaF and 1 mM sodium orthovanadate) and proteases inhibitors (1 mM PMSF, 10 μg/mL aprotinin, and 10 μg/mL leupeptin). Acidic extracts of histones were prepared as previously reported [93]. All protein extracts were quantified using the Bradford protein assay (Bio-Rad; Hercules, CA). Lysates were boiled at 100ºC in Laemmli buffer for 5 min for gel loading.

4.5. Antibodies

The antibodies used are listed in Table 1 and were diluted in TBS-0.1% Tween20 or PBS-1% BSA for immunoblots and/or immunofluorescence assays, respectively.

4.6. SDS-Page electrophoresis and western blot analysis

Proteins were fractionated by SDS-Page vertical electrophoresis and transferred to Immobilon-FL membranes (Millipore) that were blocked with TBS-T buffer (25 mM Tris-HCl (pH 8.0), 50 mM NaCl and 2.5 mM KCl, 0.1% Tween-20) and 5% nonfat dry milk, or 5% BSA (bovine serum albumin), for one hour at room temperature. Next, membranes were incubated with the primary antibody overnight at 4 °C, followed by three washes of 10 minutes in TBS-T buffer. Afterwards, membranes were incubated with the corresponding secondary antibodies for 1 hour in darkness, followed by three washes with TBS-T buffer (10 min). Finally, membrane signals were detected using the LI-COR Odyssey Infrared Imaging System (LI-COR Biosciences; Lincoln, NE, USA) [66,91,92].

4.7. Immunofluorescence and confocal microscopy

Cells were plated on 60 mm dishes which included coverslips to be used for immunofluorescence experiments [58,66,92,94,95]. Cells on coverslips were fixed with 3% paraformaldehyde for 30 minutes and treated with 200 mM glycine solution for 15 min at room temperature to eliminate the paraformaldehyde. Cells were permeabilized with 0.2 % Triton X-100 solution in PBS for 30 minutes and blocked with 1% BSA in PBS for 30 minutes at room temperature or overnight at 4ºC. For the simultaneous detection of two proteins, coverslips were sequentially incubated with the two primary antibodies, followed by three washes for 10 minutes in PBS after each one. The incubation with the corresponding secondary antibodies (Table 1), was performed for 1 hour at room temperature in darkness, and finally washed three times for 10 min in PBS. Nuclei were stained with DAPI (4′, 6′-diamidino-2-phenylindole) (Sigma), diluted 1:1000 in PBS for 15 min at room temperature, and washed three times for 10 minutes in PBS. Coverslips were mounted with Mowiol (Calbiochem-Merck, Darmstadt, Germany). Images were acquired with a LEICA SP5 DMI-6000B confocal microscope (Leica), with the following lasers: Argon (488 nm), DPSS (561 nm) and UV Diode (405 nm). These images were captured with a 63.0x lens zoomed in 1.5–3× with a 1024×1024 frame and 600 Hz scanning speed and pinhole (95.6 μm), lasers intensity and photomultipliers gain and offset were maintained constant for all samples examined. Image analysis was performed with the ImageJ software (https://imagej.nih.gov/ij/).

Table 1. List of antibodies and applications.

Primary antibodies		Dilution (WB/IF)	Clone and/or reference code	Supplier
53BP1	Rabbit polyclonal	-; 1/200	H300, sc-22760	Santa Cruz Biotechnology
53BP1	Rabbit polyclonal	1/500; 1/200	NB100-304	Novus Biologicals
γH2AX	Mouse monoclonal	-; 1/200	Clone JBW301; 05-636	Millipore
MDC1	Rabbit polyclonal	1/500; 1/200	ab11169	Abcam
NBS1	Mouse monoclonal	-; 1/200	611871	BD Biosciences
NBS1 (Nibrin)	Rabbit polyclonal	1/1000; -	N 3162	Sigma-Aldrich
PARP1	Mouse monoclonal	1/1000; -	sc-8007	Santa Cruz Biotechnology
β-actin	Mouse monoclonal	1/2000; -	AC15 / A5441	Sigma-Aldrich
Histone H4-K16ac	Rabbit monoclonal	1/500; 1/400	ab109463	Abcam
Histone H4-K20me2	Rabbit polyclonal	1/500; 1/100	9759	Cell Signaling
Cleaved caspase 3	Rabbit monoclonal	1/1000; -	5A1E / 9664	Cell Signaling
Secondary antibodies		**Dilution (WB/IF)**	**Reference code**	**Supplier**
Anti-mouse IgG (WB)	Goat Anti-Mouse IgG, DyLight 680 (red)	1/10000; -	35518	Thermo Scientific
Anti-rabbit IgG (WB)	Goat Anti-Rabbit IgG, DyLight 800 (green)	1/10000; -	35571	Thermo Scientific
Goat anti-Mouse IgG (IF)	Goat anti-Mouse IgG linked to Cy3 (red)	-; 1/1000	115-165-146	Jackson ImmunoResearch
Goat anti-rabbit IgG (IF)	Goat anti-rabbit IgG linked to Cy2 (green)	-; 1/1000	111-225-144	Jackson ImmunoResearch

4.8. Statistical analysis

The IBM SPSS 25 statistics package was used for analysis. Statistical significance was calculated using Mann-Whitney U tests, which analyze differences between only two pairs of samples, or Dunn's multiple comparison tests whether more than two samples were assessed at the same time, and not all of them were adjusted to a normal distribution [96].

5. Conclusion

The inhibition of KMTs by chaetocin or tazemetostat causes a significant reduction of H4K20me2 levels, which impairs the recruitment and formation of 53BP1 foci induced by DNA damage. As a consequence of this defective DDR, there is an increase in DNA damage that promotes tumor cell death. Based on these effects, we propose that new therapeutic approaches against tumor cells can be based on the use of these KMT inhibitors in synthetic lethality strategies to treat cancer.

Ethics approval and consent to participate

Not applicable

Consent for publication

All authors have read the manuscript and indicated their consent for publication.

Availability of data and material

All materials are available upon request. No datasets have been generated or used in this article.

Supplementary information: The following are available online at www.mdpi.com/xxx/s1, **Figure S1**: Chaetocin impairs 53BP1 foci formation induced by IR in U2OS osteosarcoma cells deprived of serum. **Figure S2**: Chaetocin impairs the assembly of 53BP1 foci induced by IR in SK-LMS-1 leiomyosarcoma serum-deprived cells. **Figure S3**: The impairment of 53BP1 foci formation caused by chaetocin is independently of the post-irradiation time in U2OS cells. **Figure S4**: Effect of chaetocin on H4K20me2 induced by IR or doxorubicin. **Figure S5**: Effect of chaetocin on the acetylation of histone H4 in lysine 16 (H4K16ac) in U2OS cells treated with IR. **Figure S6**: Effect of tazemetostat on γH2AX and 53BP1 foci in response to doxorubicin treatment in U2OS osteosarcoma cells deprived of serum. **Figure S7**: Effect of tazemetostat on γH2AX and 53BP1 foci in response to doxorubicin treatment in SK-LMS-1 leiomyosarcoma cells. **Figure S8**: The assembly of 53BP1 foci is not affected by JMJD2i treatment, a KDM inhibitor, after inducing DSBs with IR in U2OS cells. **Figure S9**: Chaetocin induces apoptotic PARP1 cleavage in response to DNA damage caused by IR in sarcoma cells. **Table S1**: Reagents used in this work.

Author contributions

ICM performed experiments, analyzed data and wrote the manuscript. RGG, ENC and EMS performed experiments, and PAL designed and coordinated this work, analyzed data and wrote the manuscript.

Funding

I.C.-M. was supported by FPI-MINECO-FSE contract (BES-2014-067721). E. M.-S. was funded by Consejería de Educación-Junta de Castilla y León (CSI004-18). E.N.-C. was funded by FPI-MINECO-FSE contract (BES-2017-080543). R.G-G was supported by Consejería de Educación-Junta de Castilla y León. This work was supported by grants from Agencia Estatal de Investigación-Ministerio de Ciencia, Innovación y Universidades-FEDER (SAF2016-75744-R, PID2019-105610RB-I00), and Consejería de Educación de la Junta de Castilla y León (CSI264P20, CLC-2017-01) to P. A. L.

Institutional Review Board Statement: Not applicable.

Acknowledgments: Atanasio Pandiella and Azucena Esparís for providing us with the SL-LMS1 cells.

Informed Consent Statement: Not applicable.

Conflicts of Interest: The funders had no role in the design of the study, collection, analyses or interpretation of data, the writing of the manuscript or the decision to publish the results.

References

1. Becker, P.B.; Workman, J.L. Nucleosome remodeling and epigenetics. *Cold Spring Harb Perspect Biol* **2013**, *5*, a017905, doi:10.1101/cshperspect.a017905.
2. Hauer, M.H.; Gasser, S.M. Chromatin and nucleosome dynamics in DNA damage and repair. *Genes Dev* **2017**, *31*, 2204-2221, doi:10.1101/gad.307702.117.
3. Ehrenhofer-Murray, A.E. Chromatin dynamics at DNA replication, transcription and repair. *Eur J Biochem* **2004**, *271*, 2335-2349, doi:10.1111/j.1432-1033.2004.04162.x.
4. Kouzarides, T. Chromatin modifications and their function. *Cell* **2007**, *128*, 693-705, doi:10.1016/j.cell.2007.02.005.
5. Kulis, M.; Esteller, M. DNA methylation and cancer. *Adv Genet* **2010**, *70*, 27-56, doi:10.1016/B978-0-12-380866-0.60002-2.
6. Dawson, M.A.; Kouzarides, T. Cancer epigenetics: from mechanism to therapy. *Cell* **2012**, *150*, 12-27, doi:10.1016/j.cell.2012.06.013.
7. Shilatifard, A. Chromatin modifications by methylation and ubiquitination: implications in the regulation of gene expression. *Annu Rev Biochem* **2006**, *75*, 243-269, doi:10.1146/annurev.biochem.75.103004.142422.
8. DesJarlais, R.; Tummino, P.J. Role of Histone-Modifying Enzymes and Their Complexes in Regulation of Chromatin Biology. *Biochemistry* **2016**, *55*, 1584-1599, doi:10.1021/acs.biochem.5b01210.
9. Wang, Z.; Patel, D.J. Small molecule epigenetic inhibitors targeted to histone lysine methyltransferases and demethylases. *Q Rev Biophys* **2013**, *46*, 349-373, doi:10.1017/S0033583513000085.
10. Toh, T.B.; Lim, J.J.; Chow, E.K. Epigenetics in cancer stem cells. *Mol Cancer* **2017**, *16*, 29, doi:10.1186/s12943-017-0596-9.
11. Greiner, D.; Bonaldi, T.; Eskeland, R.; Roemer, E.; Imhof, A. Identification of a specific inhibitor of the histone methyltransferase SU(VAR)3-9. *Nat Chem Biol* **2005**, *1*, 143-145, doi:10.1038/nchembio721.
12. Chaib, H.; Nebbioso, A.; Prebet, T.; Castellano, R.; Garbit, S.; Restouin, A.; Vey, N.; Altucci, L.; Collette, Y. Anti-leukemia activity of chaetocin via death receptor-dependent apoptosis and dual modulation of the histone methyl-transferase SUV39H1. *Leukemia* **2012**, *26*, 662-674, doi:10.1038/leu.2011.271.
13. Lai, Y.S.; Chen, J.Y.; Tsai, H.J.; Chen, T.Y.; Hung, W.C. The SUV39H1 inhibitor chaetocin induces differentiation and shows synergistic cytotoxicity with other epigenetic drugs in acute myeloid leukemia cells. *Blood Cancer J* **2015**, *5*, e313, doi:10.1038/bcj.2015.37.

14. Iwasa, E.; Hamashima, Y.; Fujishiro, S.; Higuchi, E.; Ito, A.; Yoshida, M.; Sodeoka, M. Total synthesis of (+)-chaetocin and its analogues: their histone methyltransferase G9a inhibitory activity. *J Am Chem Soc* **2010**, *132*, 4078-4079, doi:10.1021/ja101280p.
15. Cherblanc, F.L.; Chapman, K.L.; Brown, R.; Fuchter, M.J. Chaetocin is a nonspecific inhibitor of histone lysine methyltransferases. *Nat Chem Biol* **2013**, *9*, 136-137, doi:10.1038/nchembio.1187.
16. Tibodeau, J.D.; Benson, L.M.; Isham, C.R.; Owen, W.G.; Bible, K.C. The anticancer agent chaetocin is a competitive substrate and inhibitor of thioredoxin reductase. *Antioxid Redox Signal* **2009**, *11*, 1097-1106, doi:10.1089/ARS.2008.2318.
17. Ciccia, A.; Elledge, S.J. The DNA damage response: making it safe to play with knives. *Mol. Cell* **2010**, *40*, 179-204, doi:10.1016/j.molcel.2010.09.019.
18. Jackson, S.P.; Bartek, J. The DNA-damage response in human biology and disease. *Nature* **2009**, *461*, 1071-1078, doi:10.1038/nature08467.
19. Dixit, D.; Ghildiyal, R.; Anto, N.P.; Sen, E. Chaetocin-induced ROS-mediated apoptosis involves ATM-YAP1 axis and JNK-dependent inhibition of glucose metabolism. *Cell Death Dis* **2014**, *5*, e1212, doi:10.1038/cddis.2014.179.
20. He, J.; Chen, X.; Li, B.; Zhou, W.; Xiao, J.; He, K.; Zhang, J.; Xiang, G. Chaetocin induces cell cycle arrest and apoptosis by regulating the ROS-mediated ASK-1/JNK signaling pathways. *Oncol Rep* **2017**, *38*, 2489-2497, doi:10.3892/or.2017.5921.
21. Isham, C.R.; Tibodeau, J.D.; Jin, W.; Xu, R.; Timm, M.M.; Bible, K.C. Chaetocin: a promising new antimyeloma agent with in vitro and in vivo activity mediated via imposition of oxidative stress. *Blood* **2007**, *109*, 2579-2588, doi:10.1182/blood-2006-07-027326.
22. Han, X.; Han, Y.; Zheng, Y.; Sun, Q.; Ma, T.; Zhang, J.; Xu, L. Chaetocin induces apoptosis in human melanoma cells through the generation of reactive oxygen species and the intrinsic mitochondrial pathway, and exerts its anti-tumor activity in vivo. *PLoS One* **2017**, *12*, e0175950, doi:10.1371/journal.pone.0175950.
23. Ozyerli-Goknar, E.; Sur-Erdem, I.; Seker, F.; Cingoz, A.; Kayabolen, A.; Kahya-Yesil, Z.; Uyulur, F.; Gezen, M.; Tolay, N.; Erman, B., et al. The fungal metabolite chaetocin is a sensitizer for pro-apoptotic therapies in glioblastoma. *Cell Death Dis* **2019**, *10*, 894, doi:10.1038/s41419-019-2107-y.
24. Liao, X.; Fan, Y.; Hou, J.; Chen, X.; Xu, X.; Yang, Y.; Shen, J.; Mi, P.; Huang, X.; Zhang, W., et al. Identification of Chaetocin as a Potent non-ROS-mediated Anticancer Drug Candidate for Gastric Cancer. *J Cancer* **2019**, *10*, 3678-3690, doi:10.7150/jca.32803.
25. Li, Z.; Huang, L.; Wei, L.; Hou, Z.; Ye, W.; Huang, S. Chaetocin induces caspase-dependent apoptosis in ovarian cancer cells via the generation of reactive oxygen species. *Oncol Lett* **2019**, *18*, 1915-1921, doi:10.3892/ol.2019.10507.
26. Liu, X.; Guo, S.; Liu, X.; Su, L. Chaetocin induces endoplasmic reticulum stress response and leads to death receptor 5-dependent apoptosis in human non-small cell lung cancer cells. *Apoptosis* **2015**, *20*, 1499-1507, doi:10.1007/s10495-015-1167-4.
27. Rothbart, S.B.; Baylin, S.B. Epigenetic Therapy for Epithelioid Sarcoma. *Cell* **2020**, *181*, 211, doi:10.1016/j.cell.2020.03.042.
28. Italiano, A. Targeting epigenetics in sarcomas through EZH2 inhibition. *J Hematol Oncol* **2020**, *13*, 33, doi:10.1186/s13045-020-00868-4.
29. Couto, C.A.; Wang, H.Y.; Green, J.C.; Kiely, R.; Siddaway, R.; Borer, C.; Pears, C.J.; Lakin, N.D. PARP regulates nonhomologous end joining through retention of Ku at double-strand breaks. *J Cell Biol* **2011**, *194*, 367-375, doi:10.1083/jcb.201012132.
30. Caron, M.C.; Sharma, A.K.; O'Sullivan, J.; Myler, L.R.; Ferreira, M.T.; Rodrigue, A.; Coulombe, Y.; Ethier, C.; Gagne, J.P.; Langelier, M.F., et al. Poly(ADP-ribose) polymerase-1 antagonizes DNA resection at double-strand breaks. *Nat Commun* **2019**, *10*, 2954, doi:10.1038/s41467-019-10741-9.
31. McMahon, M.; Frangova, T.G.; Henderson, C.J.; Wolf, C.R. Olaparib, Monotherapy or with Ionizing Radiation, Exacerbates DNA Damage in Normal Tissues: Insights from a New p21 Reporter Mouse. *Mol Cancer Res* **2016**, *14*, 1195-1203, doi:10.1158/1541-7786.MCR-16-0108.

32. Lee, H.J.; Yoon, C.; Schmidt, B.; Park, D.J.; Zhang, A.Y.; Erkizan, H.V.; Toretsky, J.A.; Kirsch, D.G.; Yoon, S.S. Combining PARP1 inhibition and radiation in Ewing sarcoma results in lethal DNA damage. *Mol Cancer Ther* **2013**, *12*, 2591-2600, doi:10.1158/1535-7163.MCT-13-0338.
33. d'Adda di Fagagna, F. Living on a break: cellular senescence as a DNA-damage response. *Nat Rev Cancer* **2008**, *8*, 512-522.
34. Ball, A.R., Jr.; Yokomori, K. Damage site chromatin: open or closed? *Curr Opin Cell Biol* **2011**, *23*, 277-283, doi:10.1016/j.ceb.2011.03.012.
35. Bakkenist, C.J.; Kastan, M.B. Chromatin perturbations during the DNA damage response in higher eukaryotes. *DNA Repair (Amst)* **2015**, *36*, 8-12, doi:10.1016/j.dnarep.2015.09.002.
36. Polo, S.E. Reshaping chromatin after DNA damage: the choreography of histone proteins. *J Mol Biol* **2015**, *427*, 626-636, doi:10.1016/j.jmb.2014.05.025.
37. Campillo-Marcos, I.; García-González, R.; Navarro-Carrasco, E.; Lazo, P.A. The human VRK1 chromatin kinase in cancer biology. *Cancer Lett* **2021**, *503*, 117-128, doi:10.1016/j.canlet.2020.12.032.
38. Deem, A.K.; Li, X.; Tyler, J.K. Epigenetic regulation of genomic integrity. *Chromosoma* **2012**, *121*, 131-151, doi:10.1007/s00412-011-0358-1.
39. Garcia-Gonzalez, R.; Morejon-Garcia, P.; Campillo-Marcos, I.; Salzano, M.; Lazo, P.A. VRK1 Phosphorylates Tip60/KAT5 and Is Required for H4K16 Acetylation in Response to DNA Damage. *Cancers (Basel)* **2020**, *12*, 2986, doi:10.3390/cancers12102986.
40. Murr, R.; Loizou, J.I.; Yang, Y.G.; Cuenin, C.; Li, H.; Wang, Z.Q.; Herceg, Z. Histone acetylation by Trrap-Tip60 modulates loading of repair proteins and repair of DNA double-strand breaks. *Nat. Cell. Biol.* **2006**, *8*, 91-99, doi:10.1038/ncb1343.
41. Pei, H.; Zhang, L.; Luo, K.; Qin, Y.; Chesi, M.; Fei, F.; Bergsagel, P.L.; Wang, L.; You, Z.; Lou, Z. MMSET regulates histone H4K20 methylation and 53BP1 accumulation at DNA damage sites. *Nature* **2011**, *470*, 124-128, doi:10.1038/nature09658.
42. Wakeman, T.P.; Wang, Q.; Feng, J.; Wang, X.F. Bat3 facilitates H3K79 dimethylation by DOT1L and promotes DNA damage-induced 53BP1 foci at G1/G2 cell-cycle phases. *EMBO J* **2012**, *31*, 2169-2181, doi:10.1038/emboj.2012.50.
43. Zhao, B.; Rothenberg, E.; Ramsden, D.A.; Lieber, M.R. The molecular basis and disease relevance of non-homologous DNA end joining. *Nature Reviews Molecular Cell Biology* **2020**, *21*, 765-781, doi:10.1038/s41580-020-00297-8.
44. Panier, S.; Boulton, S.J. Double-strand break repair: 53BP1 comes into focus. *Nat Rev Mol Cell Biol* **2014**, *15*, 7-18, doi:10.1038/nrm3719.
45. Lottersberger, F.; Bothmer, A.; Robbiani, D.F.; Nussenzweig, M.C.; de Lange, T. Role of 53BP1 oligomerization in regulating double-strand break repair. *Proc Natl Acad Sci U S A* **2013**, *110*, 2146-2151, doi:10.1073/pnas.1222617110.
46. Shibata, A. Regulation of repair pathway choice at two-ended DNA double-strand breaks. *Mutat Res* **2017**, *803-805*, 51-55, doi:10.1016/j.mrfmmm.2017.07.011.
47. Dulev, S.; Tkach, J.; Lin, S.; Batada, N.N. SET8 methyltransferase activity during the DNA double-strand break response is required for recruitment of 53BP1. *EMBO Rep* **2014**, *15*, 1163-1174, doi:10.15252/embr.201439434.
48. Pei, D.; Zhang, Y.; Zheng, J. Regulation of p53: a collaboration between Mdm2 and Mdmx. *Oncotarget* **2012**, *3*, 228-235, doi:10.18632/oncotarget.443
49. Li, Z.; Bao, J.; Qi, Y.; Zhang, J.Z.H. Computational approaches to studying methylated H4K20 recognition by DNA repair factor 53BP1. *Phys Chem Chem Phys* **2020**, *22*, 6136-6144, doi:10.1039/c9cp05635a.
50. Bunting, S.F.; Callen, E.; Wong, N.; Chen, H.T.; Polato, F.; Gunn, A.; Bothmer, A.; Feldhahn, N.; Fernandez-Capetillo, O.; Cao, L., et al. 53BP1 inhibits homologous recombination in Brca1-deficient cells by blocking resection of DNA breaks. *Cell* **2010**, *141*, 243-254, doi:10.1016/j.cell.2010.03.012.
51. Wheeler, D.A.; Takebe, N.; Hinoue, T.; Hoadley, K.A.; Cardenas, M.F.; Hamilton, A.M.; Laird, P.W.; Wang, L.; Johnson, A.; Dewal, N., et al. Molecular Features of Cancers Exhibiting Exceptional Responses to Treatment. *Cancer Cell* **2021**, *39*, 1-16, doi:10.1016/j.ccell.2020.10.015.

52. D'Ambrosio, L.; Touati, N.; Blay, J.Y.; Grignani, G.; Flippot, R.; Czarnecka, A.M.; Piperno-Neumann, S.; Martin-Broto, J.; Sanfilippo, R.; Katz, D., et al. Doxorubicin plus dacarbazine, doxorubicin plus ifosfamide, or doxorubicin alone as a first-line treatment for advanced leiomyosarcoma: A propensity score matching analysis from the European Organization for Research and Treatment of Cancer Soft Tissue and Bone Sarcoma Group. *Cancer* **2020**, *126*, 2637-2647, doi:10.1002/cncr.32795.
53. Kaelin, W.G., Jr. The concept of synthetic lethality in the context of anticancer therapy. *Nat Rev Cancer* **2005**, *5*, 689-698, doi:10.1038/nrc1691.
54. Huang, A.; Garraway, L.A.; Ashworth, A.; Weber, B. Synthetic lethality as an engine for cancer drug target discovery. *Nat Rev Drug Discov* **2020**, *19*, 23-38, doi:10.1038/s41573-019-0046-z.
55. Maurel, J.; Lopez-Pousa, A.; de Las Penas, R.; Fra, J.; Martin, J.; Cruz, J.; Casado, A.; Poveda, A.; Martinez-Trufero, J.; Balana, C., et al. Efficacy of sequential high-dose doxorubicin and ifosfamide compared with standard-dose doxorubicin in patients with advanced soft tissue sarcoma: an open-label randomized phase II study of the Spanish group for research on sarcomas. *J Clin Oncol* **2009**, *27*, 1893-1898.
56. van Attikum, H.; Gasser, S.M. The histone code at DNA breaks: a guide to repair? *Nat Rev Mol Cell Biol* **2005**.
57. Bekker-Jensen, S.; Mailand, N. Assembly and function of DNA double-strand break repair foci in mammalian cells. *DNA Repair (Amst)* **2010**, *9*, 1219-1228, doi:10.1016/j.dnarep.2010.09.010.
58. Salzano, M.; Sanz-Garcia, M.; Monsalve, D.M.; Moura, D.S.; Lazo, P.A. VRK1 chromatin kinase phosphorylates H2AX and is required for foci formation induced by DNA damage. *Epigenetics* **2015**, *10*, 373-383, doi:10.1080/15592294.2015.1028708.
59. Mirman, Z.; de Lange, T. 53BP1: a DSB escort. *Genes Dev* **2020**, *34*, 7-23, doi:10.1101/gad.333237.119.
60. Fong, P.C.; Boss, D.S.; Yap, T.A.; Tutt, A.; Wu, P.; Mergui-Roelvink, M.; Mortimer, P.; Swaisland, H.; Lau, A.; O'Connor, M.J., et al. Inhibition of poly(ADP-ribose) polymerase in tumors from BRCA mutation carriers. *N Engl J Med* **2009**, *361*, 123-134, doi:10.1056/NEJMoa0900212.
61. Fong, P.C.; Yap, T.A.; Boss, D.S.; Carden, C.P.; Mergui-Roelvink, M.; Gourley, C.; De Greve, J.; Lubinski, J.; Shanley, S.; Messiou, C., et al. Poly(ADP)-ribose polymerase inhibition: frequent durable responses in BRCA carrier ovarian cancer correlating with platinum-free interval. *J Clin Oncol* **2010**, *28*, 2512-2519, doi:10.1200/JCO.2009.26.9589.
62. Shimada, K.; Yamaguchi, M.; Atsuta, Y.; Matsue, K.; Sato, K.; Kusumoto, S.; Nagai, H.; Takizawa, J.; Fukuhara, N.; Nagafuji, K., et al. Rituximab, cyclophosphamide, doxorubicin, vincristine, and prednisolone combined with high-dose methotrexate plus intrathecal chemotherapy for newly diagnosed intravascular large B-cell lymphoma (PRIMEUR-IVL): a multicentre, single-arm, phase 2 trial. *Lancet Oncol* **2020**, *21*, 593-602, doi:10.1016/S1470-2045(20)30059-0.
63. Lord, C.J.; Ashworth, A. PARP inhibitors: Synthetic lethality in the clinic. *Science* **2017**, *355*, 1152-1158, doi:10.1126/science.aam7344.
64. Eliezer, Y.; Argaman, L.; Rhie, A.; Doherty, A.J.; Goldberg, M. The direct interaction between 53BP1 and MDC1 is required for the recruitment of 53BP1 to sites of damage. *J Biol Chem* **2009**, *284*, 426-435, doi:10.1074/jbc.M807375200.
65. Lavin, M.F.; Kozlov, S.; Gatei, M.; Kijas, A.W. ATM-Dependent Phosphorylation of All Three Members of the MRN Complex: From Sensor to Adaptor. *Biomolecules* **2015**, *5*, 2877-2902, doi:10.3390/biom5042877.
66. Monsalve, D.M.; Campillo-Marcos, I.; Salzano, M.; Sanz-Garcia, M.; Cantarero, L.; Lazo, P.A. VRK1 phosphorylates and protects NBS1 from ubiquitination and proteasomal degradation in response to DNA damage. *Biochim Biophys Acta, Molecular Cell Research* **2016**, *1863*, 760-769, doi:10.1016/j.bbamcr.2016.02.005.
67. Wilson, M.D.; Benlekbir, S.; Fradet-Turcotte, A.; Sherker, A.; Julien, J.P.; McEwan, A.; Noordermeer, S.M.; Sicheri, F.; Rubinstein, J.L.; Durocher, D. The structural basis of modified nucleosome recognition by 53BP1. *Nature* **2016**, *536*, 100-103, doi:10.1038/nature18951.
68. Li, L.; Wang, Y. Cross-talk between the H3K36me3 and H4K16ac histone epigenetic marks in DNA double-strand break repair. *J Biol Chem* **2017**, *292*, 11951-11959, doi:10.1074/jbc.M117.788224.
69. Hsiao, K.Y.; Mizzen, C.A. Histone H4 deacetylation facilitates 53BP1 DNA damage signaling and double-strand break repair. *J Mol Cell Biol* **2013**, *5*, 157-165, doi:10.1093/jmcb/mjs066.

70. Dockerill, M.; Gregson, C.; DH, O.D. Targeting PRC2 for the treatment of cancer: an updated patent review (2016 - 2020). *Expert Opin Ther Pat* **2020**, 10.1080/13543776.2021.1841167, doi:10.1080/13543776.2021.1841167.
71. Soumyanarayanan, U.; Dymock, B.W. Recently discovered EZH2 and EHMT2 (G9a) inhibitors. *Future Med Chem* **2016**, *8*, 1635-1654, doi:10.4155/fmc-2016-0096.
72. Gounder, M.; Schoffski, P.; Jones, R.L.; Agulnik, M.; Cote, G.M.; Villalobos, V.M.; Attia, S.; Chugh, R.; Chen, T.W.; Jahan, T., et al. Tazemetostat in advanced epithelioid sarcoma with loss of INI1/SMARCB1: an international, open-label, phase 2 basket study. *Lancet Oncol* **2020**, *21*, 1423-1432, doi:10.1016/S1470-2045(20)30451-4.
73. Chan, E.M.; Shibue, T.; McFarland, J.M.; Gaeta, B.; Ghandi, M.; Dumont, N.; Gonzalez, A.; McPartlan, J.S.; Li, T.; Zhang, Y., et al. WRN helicase is a synthetic lethal target in microsatellite unstable cancers. *Nature* **2019**, *568*, 551-556, doi:10.1038/s41586-019-1102-x.
74. Kategaya, L.; Perumal, S.K.; Hager, J.H.; Belmont, L.D. Werner Syndrome Helicase Is Required for the Survival of Cancer Cells with Microsatellite Instability. *iScience* **2019**, *13*, 488-497, doi:10.1016/j.isci.2019.02.006.
75. Lieb, S.; Blaha-Ostermann, S.; Kamper, E.; Rippka, J.; Schwarz, C.; Ehrenhofer-Wolfer, K.; Schlattl, A.; Wernitznig, A.; Lipp, J.J.; Nagasaka, K., et al. Werner syndrome helicase is a selective vulnerability of microsatellite instability-high tumor cells. *Elife* **2019**, *8*, e43333, doi:10.7554/eLife.43333.
76. Tewari, K.S.; Eskander, R.N.; Monk, B.J. Development of Olaparib for BRCA-Deficient Recurrent Epithelial Ovarian Cancer. *Clin Cancer Res* **2015**, *21*, 3829-3835, doi:10.1158/1078-0432.CCR-15-0088.
77. Leichman, L.; Groshen, S.; O'Neil, B.H.; Messersmith, W.; Berlin, J.; Chan, E.; Leichman, C.G.; Cohen, S.J.; Cohen, D.; Lenz, H.J., et al. Phase II Study of Olaparib (AZD-2281) After Standard Systemic Therapies for Disseminated Colorectal Cancer. *Oncologist* **2016**, *21*, 172-177, doi:10.1634/theoncologist.2015-0319.
78. Srinivasan, G.; Sidhu, G.S.; Williamson, E.A.; Jaiswal, A.S.; Najmunnisa, N.; Wilcoxen, K.; Jones, D.; George, T.J., Jr.; Hromas, R. Synthetic lethality in malignant pleural mesothelioma with PARP1 inhibition. *Cancer Chemother Pharmacol* **2017**, *80*, 861-867, doi:10.1007/s00280-017-3401-y.
79. Jacquet, K.; Fradet-Turcotte, A.; Avvakumov, N.; Lambert, J.P.; Roques, C.; Pandita, R.K.; Paquet, E.; Herst, P.; Gingras, A.C.; Pandita, T.K., et al. The TIP60 Complex Regulates Bivalent Chromatin Recognition by 53BP1 through Direct H4K20me Binding and H2AK15 Acetylation. *Mol Cell* **2016**, *62*, 409-421, doi:10.1016/j.molcel.2016.03.031.
80. Lou, Z.; Minter-Dykhouse, K.; Franco, S.; Gostissa, M.; Rivera, M.A.; Celeste, A.; Manis, J.P.; van Deursen, J.; Nussenzweig, A.; Paull, T.T., et al. MDC1 maintains genomic stability by participating in the amplification of ATM-dependent DNA damage signals. *Mol Cell* **2006**, *21*, 187-200, doi:10.1016/j.molcel.2005.11.025.
81. Liu, J.; Luo, S.; Zhao, H.; Liao, J.; Li, J.; Yang, C.; Xu, B.; Stern, D.F.; Xu, X.; Ye, K. Structural mechanism of the phosphorylation-dependent dimerization of the MDC1 forkhead-associated domain. *Nucleic Acids Res* **2012**, *40*, 3898-3912, doi:10.1093/nar/gkr1296.
82. Brach, D.; Johnston-Blackwell, D.; Drew, A.; Lingaraj, T.; Motwani, V.; Warholic, N.M.; Feldman, I.; Plescia, C.; Smith, J.J.; Copeland, R.A., et al. EZH2 Inhibition by Tazemetostat Results in Altered Dependency on B-cell Activation Signaling in DLBCL. *Mol Cancer Ther* **2017**, *16*, 2586-2597, doi:10.1158/1535-7163.MCT-16-0840.
83. Italiano, A.; Soria, J.C.; Toulmonde, M.; Michot, J.M.; Lucchesi, C.; Varga, A.; Coindre, J.M.; Blakemore, S.J.; Clawson, A.; Suttle, B., et al. Tazemetostat, an EZH2 inhibitor, in relapsed or refractory B-cell non-Hodgkin lymphoma and advanced solid tumours: a first-in-human, open-label, phase 1 study. *Lancet Oncol* **2018**, *19*, 649-659, doi:10.1016/S1470-2045(18)30145-1.
84. Tang, J.; Cho, N.W.; Cui, G.; Manion, E.M.; Shanbhag, N.M.; Botuyan, M.V.; Mer, G.; Greenberg, R.A. Acetylation limits 53BP1 association with damaged chromatin to promote homologous recombination. *Nat Struct Mol Biol* **2013**, *20*, 317-325, doi:10.1038/nsmb.2499.

85. Wen, C.; Wang, H.; Wu, X.; He, L.; Zhou, Q.; Wang, F.; Chen, S.; Huang, L.; Chen, J.; Wang, H., et al. ROS-mediated inactivation of the PI3K/AKT pathway is involved in the antigastric cancer effects of thioredoxin reductase-1 inhibitor chaetocin. *Cell Death Dis* **2019**, *10*, 809, doi:10.1038/s41419-019-2035-x.
86. Hoeijmakers, J.H. Genome maintenance mechanisms for preventing cancer. *Nature* **2001**, *411*, 366-374, doi:10.1038/35077232.
87. van Gent, D.C.; Hoeijmakers, J.H.; Kanaar, R. Chromosomal stability and the DNA double-stranded break connection. *Nat Rev Genet* **2001**, *2*, 196-206, doi:10.1038/35056049.
88. Bruner, S.D.; Norman, D.P.; Verdine, G.L. Structural basis for recognition and repair of the endogenous mutagen 8-oxoguanine in DNA. *Nature* **2000**, *403*, 859-866, doi:10.1038/35002510.
89. Soldani, C.; Scovassi, A.I. Poly(ADP-ribose) polymerase-1 cleavage during apoptosis: an update. *Apoptosis* **2002**, *7*, 321-328, doi:10.1023/a:1016119328968.
90. Duriez, P.J.; Shah, G.M. Cleavage of poly(ADP-ribose) polymerase: a sensitive parameter to study cell death. *Biochem Cell Biol* **1997**, *75*, 337-349.
91. Sanz-Garcia, M.; Monsalve, D.M.; Sevilla, A.; Lazo, P.A. Vaccinia-related Kinase 1 (VRK1) is an upstream nucleosomal kinase required for the assembly of 53BP1 foci in response to ionizing radiation-induced DNA damage. *J. Biol. Chem.* **2012**, *287*, 23757-23768, doi:10.1074/jbc.M112.353102.
92. Campillo-Marcos, I.; Lazo, P.A. Olaparib and ionizing radiation trigger a cooperative DNA-damage repair response that is impaired by depletion of the VRK1 chromatin kinase. *J Exp Clin Cancer Res* **2019**, *38*, 203, doi:10.1186/s13046-019-1204-1.
93. Shechter, D.; Dormann, H.L.; Allis, C.D.; Hake, S.B. Extraction, purification and analysis of histones. *Nat. Protoc.* **2007**, *2*, 1445-1457, doi:10.1038/nprot.2007.202.
94. Salzano, M.; Vazquez-Cedeira, M.; Sanz-Garcia, M.; Valbuena, A.; Blanco, S.; Fernandez, I.F.; Lazo, P.A. Vaccinia-related kinase 1 (VRK1) confers resistance to DNA-damaging agents in human breast cancer by affecting DNA damage response. *Oncotarget* **2014**, *5*, 1770-1778, doi:10.18632/oncotarget.1678.
95. Moura, D.S.; Campillo-Marcos, I.; Vazquez-Cedeira, M.; Lazo, P.A. VRK1 and AURKB form a complex that cross inhibit their kinase activity and the phosphorylation of histone H3 in the progression of mitosis. *Cell Mol Life Sci* **2018**, *76*, 2591-2611, doi:10.1007/s00018-018-2746-7.
96. Bremer, M.; Doerge, R.M. Statistics at the bench: a step-by step handbook for biologists; Cold Spring Harbor Laboratory Press: New York, 2009.